

CERN/EP/83-97  
22 July 1983G(1590), A SCALAR MESON DECAYING INTO TWO  $\eta$ -MESONSIHEP<sup>1</sup>-IISN<sup>2</sup>-LAPP<sup>3</sup> Collaboration

F. Binon<sup>2</sup>, S.V. Donskov<sup>1</sup>, P. Duteil<sup>4</sup>, M. Gouanère<sup>3</sup>,  
 A.V. Inyakin<sup>1</sup>, V.A. Kachanov<sup>1</sup>, D.B. Kakauridze<sup>1</sup>, G.V. Khaustov<sup>1</sup>,  
 A.V. Kulik<sup>1</sup>, J.P. Lagnaux<sup>2</sup>, A.A. Lednev<sup>1</sup>, Yu.V. Mikhailov<sup>1</sup>,  
 J.P. Peigneux<sup>3</sup>, Yu.D. Prokoshkin<sup>1</sup>, Yu.V. Rodnov<sup>1</sup>, S.A. Sadovsky<sup>1</sup>,  
 A.V. Singovsky<sup>1</sup>, J.P. Stroot<sup>2</sup> and V.P. Sugonyaev<sup>1</sup>

Joint Experiment of IHEP, Serpukhov, USSR  
 and  
 CERN, Geneva, Switzerland

ABSTRACT

An experiment to search for gluonium states in  $\eta$  pairs produced in  $\pi^-p$  interactions at 38 GeV/c momentum has been performed at the 70 GeV IHEP accelerator with the hodoscope spectrometer GAMS-2000. An S-wave resonance, G(1590), has been observed. Its mass is  $(1592 \pm 25)$  MeV/c<sup>2</sup>, its width is  $(210 \pm 40)$  MeV/c<sup>2</sup>. Its quantum numbers are  $J^{PC} = 0^{++}$ ,  $I^G = 0^+$ . The decay rate into two neutral pions is at least three times lower than that of  $G \rightarrow \eta\eta$ .  $\sigma(\pi^-p \rightarrow G\eta) \cdot BR(G \rightarrow \eta\eta)$  is found to be  $(33 \pm 8) \cdot 10^{-33}$  cm<sup>2</sup>. The properties of G(1590) as a possible gluon bound state are discussed. In the same experiment the rare decay  $f \rightarrow \eta\eta$  has been observed for the first time. Its branching ratio is found to be  $BR(f \rightarrow \eta\eta) = (5.2 \pm 1.7) \cdot 10^{-3}$ .

Submitted to Nuovo Cimento

- 
- 1 Institute for High Energy Physics, Serpukhov, USSR.
  - 2 Institut Interuniversitaire des Sciences Nucléaires, Brussels, Belgium.
  - 3 Laboratoire d'Annecy de Physique des Particules, France.
  - 4 CERN, Geneva, Switzerland.

## 1. INTRODUCTION

The present experiment was aimed at the study of neutral meson states which decay into two  $\eta$ -mesons in a mass range up to  $2 \text{ GeV}/c^2$ . These states have been produced in the charge exchange reaction



$\eta\eta$  systems have been little studied up to now. They have been found in two experiments involving the NICE [1] set-up at IHEP and the Crystal Ball [2] at SLAC. In both cases the statistical accuracy was rather limited.

The interest in these studies has been raised by the discovery of the  $\theta$ -meson with a mass of about  $1.7 \text{ GeV}/c^2$  decaying into two  $\eta$  amongst the decay products of the  $J/\psi$ :  $J/\psi \rightarrow \gamma\eta\eta$  [2]. The  $\theta$ -meson may be interpreted as a gluonium (or glueball), a gluon bound state [3]. Later another decay mode of this particle has been observed:  $\theta \rightarrow K\bar{K}$  [4]. Its spin and parity are  $J^P = 2^+$ .

Systems which decay into two  $\eta$ -mesons are interesting in many respects apart from the gluonium problem. In particular, they have the following properties: (i) isospin, parity, charge conjugation and G-parity are fixed ( $I=0$ ; P, C and G are even); (ii) their spin may only be even: 0, 2, ...; (iii) the decay rate  $M^0 \rightarrow \eta\eta$  near the production threshold is proportional to  $p_0^{2J+1}$  where  $p_0$  is the  $\eta$  momentum in the  $M^0$  rest frame. As a consequence low spin dominates at low  $M^0$  mass values ( $M_{\eta\eta} < 2 \text{ GeV}/c^2$ ).

Thus the study of reaction (1) is an efficient method to search for scalar mesons ( $J^P = 0^+$ ), which is not obscured by a strong D-wave contribution as it is the case for  $M^0$  decaying into two pions in the mass region  $1 \text{ GeV}/c^2 \lesssim M_{\pi\pi} \lesssim 2 \text{ GeV}/c^2$ .

## 2. EXPERIMENTAL CONDITIONS

The measurements have been performed in a 38 GeV/c negative pion beam at the IHEP accelerator. The experimental lay-out has been described earlier [5].  $\pi^-$  are focused on a liquid hydrogen target surrounded by a counter guard system. The gamma-rays are detected with the hodoscope spectrometer GAMS-2000. The distance between the target and GAMS has been fixed at 4.4 meters so that gamma shower overlapping in the spectrometer is negligible and that events from reaction (1) are detected with high efficiency in the range of masses up to 2 GeV/c<sup>2</sup>.

The set-up is triggered on events in the exclusive production channel of neutral states decaying finally into a number k of gamma-rays

$$\pi^- + p \rightarrow k\gamma + n. \quad (2)$$

This includes reaction (1). The abundant contributions of  $\pi^-p \rightarrow \pi^0n$  and  $\pi^-p \rightarrow \eta n$  are eliminated with the help of a fast processor which only accepts events for which the mass of the  $k\gamma$  states is larger than 0.9 GeV/c<sup>2</sup>. The set-up and the measurement procedures have been described elsewhere [5-7].

10<sup>12</sup> pions in bursts of 10<sup>7</sup> per accelerator cycle have been hitting the liquid hydrogen target over a period of two weeks, giving a sensitivity of 50 events of type (1) per nanobarn. 10<sup>7</sup> events of type (2) have been recorded on magnetic tapes.

## 3. RECONSTRUCTION AND SELECTION OF EVENTS

The event reconstruction program [5,6] is looking for electromagnetic showers produced by gamma-rays in GAMS; it determines their coordinates and their energy. It dispatches the events in classes according to the number of observed gammas. Only events with 4 gamma-rays have been retained in the present analysis.

The invariant  $M_{\gamma_i\gamma_j}$  mass ( $i, j=1, \dots, 4$ ; 6 combinations per event) of each pair of gamma-rays is calculated. The mass spectrum (Fig. 1a) shows that most events are due to neutral pion pair production [8]

$$\pi^-p \rightarrow \pi^0\pi^0n \quad (3)$$

(including  $\epsilon$  and  $f$  mesons decaying into two  $\pi^0$ ).

Events in which the mass of one pair of gammas is inside the range  $450 \text{ MeV}/c^2 < M_{\gamma_1\gamma_2} < 650 \text{ MeV}/c^2$ , around the  $\eta$ -meson mass, are further considered. The spectrum of the remaining pairs  $M_{\gamma_3\gamma_4}$  is shown on Fig. 1b.

The experimental identification of the low intensity  $\eta$ -pair reaction (1) is complicated by the rather high combinatorial background (Fig. 1a) from the  $\pi^0$ -pair reaction (3) whose cross-section is 30 times larger [1]. Less confusing is the reaction  $\pi^-p \rightarrow \eta\pi^0n$  [9] which has about the same rate as (1). Events in which  $\gamma$  pairs accidentally simulate the mass of the  $\eta$ -meson still give an important background (Fig. 1b).

The further requirement for events not to include any  $\gamma$  pair with a mass between 90 and 180  $\text{MeV}/c^2$  corresponding to a  $\pi^0$ , so that only remain four-gamma events with a topology excluding a possible interpretation as  $\pi^0\pi^0$  or  $\eta\pi^0$ , drastically decreases this combinatorial background (Fig. 1c and 1d). The final selection includes 13,000 pure  $\eta\eta$  events.

The kinematical parameters of the  $\eta\eta$  events are determined in a 3C fit procedure (fixing the mass of all particles  $M_{\gamma_1\gamma_2} = M_{\gamma_3\gamma_4} = M_\eta$ ,  $E_{\eta\eta} = 38 \text{ GeV} + t/2m_n$ , where  $E_{\eta\eta}$  is the sum of the energies of the four gammas,  $m_n$  is the neutron mass and  $t$  is the four-momentum transfer squared). Events with  $\chi^2 < 10$  (98% probability) are retained for final analysis.

#### 4. MASS SPECTRUM

$\eta\eta$  events peak at small momentum transfer (Fig. 2). The shape of their  $t$ -distribution is characteristic of one pion exchange processes (OPE). The mass and decay angle distributions of the  $\eta\eta$  pairs are identical in the intervals  $|t| < 0.1 \text{ (GeV}/c)^2$  and  $|t| < 0.2 \text{ (GeV}/c)^2$ . The final analysis has been restricted to events with  $|t| < 0.2 \text{ (GeV}/c)^2$ , a  $t$  region where OPE dominates, as it is the case for reaction (3).

The mass spectrum is drawn on Fig. 3. A sharp threshold rise, typical of a S-wave behaviour, and a peak in the mass region around  $1350 \text{ MeV}/c^2$  are observed. The spectrum has been corrected for detection efficiency  $\epsilon$  of events from reaction (1).

## 5. EFFICIENCY

The efficiency as a function of the mass  $M_{\eta\eta}$  and of the spherical angles  $\theta^*$  and  $\varphi^*$  (in the Gottfried-Jackson system) has been determined by simulation with real showers collected in a data base [5]. The analysis of simulated events has been performed with the same programs which have been used for the analysis of the experimental data. In this way  $\epsilon$  may be determined with a precision of the order of one percent [5]. This procedure takes into account simultaneously the geometry of the set up (in this case the acceptance is nearly one), the efficiency of the reconstruction program and of the kinematical analysis and the relevance of the selection criteria in real experimental conditions.

The kinematics of reaction (1) in the near threshold mass range of  $M_{\eta\eta}$  favor forward emission of  $\eta$ -mesons in the laboratory coordinate system. As a result the acceptance of the spectrometer is large even at  $\cos \theta^* \approx 1$  and the efficiency  $\epsilon(M_{\eta\eta}, \theta^*, \varphi^*)$  is rather constant, varying little with mass and angles (Fig. 4).  $\epsilon$  can be well approximated by a linear combination of a few spherical harmonics:

$$\epsilon(M_{\eta\eta}, \theta^*, \varphi^*) = \sum_{\ell} [a_{\ell 0}(M_{\eta\eta}) Y_{\ell 0}(\theta^*) + 2 \sum_{m=1}^{\ell} a_{\ell m}(M_{\eta\eta}) \text{Re} Y_{\ell m}(\theta^*, \varphi^*)] \quad (4)$$

$a_{\ell m}$  coefficients are polynomials of order 3 at a maximum. In practice only coefficients with  $\ell m = 00, 20, 21, 22, 40$  or  $42$  differ from zero. The possibility of such an analytic expression for the efficiency definitely simplifies the analysis.

The mass resolution  $\sigma_M$  of the spectrometer for events in reaction (1) does not depend on the spherical angles. It varies monotonously from  $20 \text{ MeV}/c^2$  to  $30 \text{ MeV}/c^2$  in the mass interval from  $1300 \text{ MeV}/c^2$  to  $1800 \text{ MeV}/c^2$  ( $\sigma_M/M \sim 1.5\%$ ).

## 6. ANGULAR DISTRIBUTION

The polar angle distributions of  $\eta\eta$  pairs in the Gottfried-Jackson system are plotted on Fig. 4 for  $80 \text{ MeV}/c^2$  mass intervals between  $1100 \text{ MeV}/c^2$  and  $1900 \text{ MeV}/c^2$ . Detection efficiency is taken into account. These distributions change abruptly and non monotonously with increasing  $\eta\eta$  mass. This indicates a complex partial wave structure in reaction (1) in the peak region as well as at large masses in the flat part of the spectrum.

The OPE approximation without absorption has been used for a first qualitative analysis of the angular distribution. Within this framework, the spin of  $M^0$  is aligned in the Gottfried-Jackson system, i.e. there are no amplitudes with  $m$ , the projection of the orbital angular momentum, different from zero and also the nucleon non spin-flip amplitudes dominate [10].

The contribution of waves higher than S or D may be neglected in the near threshold region of reaction (1),  $1.1 \text{ GeV}/c^2 < M_{\eta\eta} < 1.9 \text{ GeV}/c^2$ . This follows from data on reaction (cf. review paper [10])



and on reaction (3) [8] where the OPE mechanism also dominates.  $\ell = 4$  waves appear in reaction (3) only at masses larger than  $1.8 \text{ GeV}/c^2$  ( $h$ -meson) [11]. It may thus be expected that the  $\ell = 4$  wave contribution to (1) near the threshold will be even smaller (with a reduction factor  $p_0^{2\ell+1}$ ).

Typical angular distributions expected for reaction (1) near the threshold are shown on Fig. 5. A pure D-wave shows a characteristic minimum at  $\cos \theta^* \approx 0.6$ . The addition of some S-wave contribution shifts the minimum to the left in case of constructive interference or to the right in case of destructive interference. In the case of a strong S-wave interfering with a D-wave, the aspect of the angular distribution changes: it either increases or decreases monotonously. These characteristic properties remain for complex S-wave and D-wave amplitudes (adding a constant contribution to the amplitude squared  $|A|^2$ ).

The data of Fig. 4 give the following general picture of the partial wave behaviour in reaction (1):

- very near threshold, only the S-wave contributes;
- later its intensity is decreasing with increasing  $M_{\eta\eta}$  and D-wave steps in and dominates in the peak region of Fig. 3;
- with  $M_{\eta\eta}$  further increasing, a strong S-wave contribution builds up (giving a typical (D+S) interference pattern) and the D-wave weakens;
- for  $M_{\eta\eta} > 1.7 \text{ GeV}/c^2$  the S-wave disappears and D-wave builds up again.

Finally, a qualitative survey of the angular distributions of reaction (1) already demonstrate that partial waves resonate, showing maxima in the region of mass around 1350 MeV/c<sup>2</sup> in D-wave and around 1600 MeV/c<sup>2</sup> in S-wave.

## 7. PARTIAL WAVES

The method of Ochs-Wagner, based on the OPE model with absorption, which has been successfully applied to the analysis of reactions (5) and (3), [10,8] and also in similar reactions with the production of K $\bar{K}$  pairs [12-14] has been used for a quantitative determination of the partial waves. In these reactions only amplitudes with  $|m| < 1$  contribute significantly. The  $D_m$ -wave contribution with  $m = \pm 1$  is accounted for by introducing a depolarisation parameter R relating it to the dominant  $D_0$ -wave:

$$D_{+1} + D_{-1} = |D_0| R e^{i(\alpha+\beta)} \quad (6)$$

where  $\alpha$  is the  $SD_0$  relative phase.

The analysis of the angular distribution of reaction (1) shows that the contribution of amplitudes with  $|m| > 1$  is not significant as the moments of  $|m| > 1$  spherical harmonics practically vanish (as also in  $\pi\pi$  and KK pair production reactions).

The angular distribution in this case is expressed as

$$\begin{aligned} N(\theta^*, \varphi^*) = & \left| |S|Y_{00} + |D_0|Y_{20}(\theta^*)e^{i\alpha} \right|^2 + R^2 \left| |D_0|Y_{21}(\theta^*, \varphi^*) \right|^2 + \\ & + R|D_0|\text{Re } Y_{21}(\theta^*, \varphi^*) [|S|Y_{00} \cos(\alpha+\beta) + |D_0|Y_{20}(\theta^*) \cos \beta] \end{aligned} \quad (7)$$

The phase  $\beta$  is put equal to  $\pi$  (phase coherence [10]).

The four real parameters  $|S|$ ,  $|D_0|$ , R and  $\alpha$  entering (7) are determined from five quantities, the moments of spherical harmonics which characterise the measured angular distribution. The problem is thus over-determined and the solution may be checked for possible contradictions.

The partial wave analysis of reaction (1) has been made according to the above described procedure in each mass interval  $\Delta M_{\eta\eta}$  independently. The values obtained for the intensity of S and  $D_0$  waves, their relative phase and the depolarisation parameter are shown on Fig. 6. Fitting the angular

distribution for a fixed value of  $R$ , leaving the phase  $\beta$  as a free parameter, the value of  $\beta$  appears to be around  $\pi$  and not much to depend on  $R$  (Fig. 6e, obtained with  $R^2 = 0.4$ ). The value of the parameters  $|S|$ ,  $|D_0|$  and  $\alpha$  are the same in both fits.

In the foregoing procedure, it was supposed that  $\ell > 4$  wave contributions to reaction (1) in the observed mass range, as well as in reactions (3) and (5), could be neglected. As a test, the analysis was repeated with a  $\ell = 4$  wave contribution. This appears to be definitely small and compatible with zero within the precision of the measurements. Results for  $|S|$ ,  $|D_0|$  and  $\alpha$  remain the same as on Fig. 6.

The partial wave analysis puts in evidence two resonances in the observed mass region in agreement with the formerly reported qualitative behaviour of angular distributions.

A clear peak at about  $1.6 \text{ GeV}/c^2$  is observed in S-wave, indicating the production of a new scalar meson (for which the denomination  $G(1590)$  will be used) decaying into two  $\eta$ -mesons. The interpretation of this state as a  $\eta\eta$  resonance is enforced by the observation of the fast variation of the phase  $\alpha$  in the region of the  $G(1590)$ .

Another resonant structure is clearly seen in the D-wave. It corresponds to the rare decay of

$$f(1270) \rightarrow \eta\eta \quad (8)$$

which had not been observed up to now. The peak is displaced to the right ( $1400 \text{ MeV}/c^2$ ) of the tabulated value of the  $f$ -meson mass. This shift is due to a factor  $p_0^{2\ell+1} = p_0^5$ . Such an effect is also seen in the decay  $f \rightarrow K^+K^-$  [12]. The phase variation in the region of the  $f$ -peak is typical for a resonant state.

## 8. PARAMETERS OF THE RESONANCES

Independent fits of S and D waves have been performed in order to evaluate the mass of the new resonance and its production cross-section. The S-wave intensity in the region of the  $G$ -meson is well described by the Breit-Wigner formula:



$$|S|^2 = \left[ \frac{A_G}{(M-M_G)^2 + \Gamma_G^2/4} + Q(M) \right] \frac{p_0(M)}{p_0(M_G)} \quad (9)$$

where, here and below,  $M$  stands for  $M_{\eta\eta}$ . Both a gaussian distribution and a polynomial function have been used for the function  $Q(M)$  describing the near threshold structure.

Formula (9) describes the experimentally observed dependence correctly (Fig. 6a). Fits for both  $Q(M)$  parametrisations are very similar, giving equal mass and width values for the  $G$ -meson:

$$M_G = (1592 \pm 25)\text{MeV}/c^2, \quad \Gamma_G = (210 \pm 40)\text{MeV}/c^2 \quad (10)$$

taking the spectrometer resolution into account.

The quantum numbers of the  $G(1590)$ -meson follow from the properties of the  $\eta\eta$  system:

$$J^{PC} = 0^{++}; \quad I^G = 0^+ \quad (11)$$

The  $D$ -wave intensity is described by a Breit-Wigner function with a dynamical width and a constant background  $C$ :

$$|D_0|^2 = \left[ \frac{F(M)}{(M^2-M_f^2)^2 + M_f^2 \Gamma^2(M)} + C \right] \frac{p_0^5(M)}{p_0^5(M_f)} \quad (12)$$

The variation of the width with the mass is given by the expression  $\Gamma(M) = \Gamma_f [p_0^\pi(M)/p_0^\pi(M_f)]^5$  where  $p_0^\pi(M) = (M^2 - 4m_\pi^2)^{1/2}/2$  is the momentum of the pion in the  $M^0$  rest frame. The form factor  $F(M)$  is obtained by analogy with a similar parametrisation for the decay  $f \rightarrow \pi^0\pi^0$ . Formula (12) gives a good description of the  $D_0$ -wave (Fig. 6b).

Another parametrisation has been tried, replacing the Breit-Wigner expression and the form factor by a gaussian function, which also gives a fast decrease far from the resonance. Fitting curves coincide for both parametrisations. A difference only appears at the background level under the  $f$ -meson peak ( $\sim 10\%$ ).

The values of the mass  $M_f = (1284 \pm 30) \text{ MeV}/c^2$  and of the width  $\Gamma_f = (240 \pm 40) \text{ MeV}/c^2$  obtained in the fit are in agreement with the  $f(1270)$  tabulated data [15]. The observed displacement of the  $f$  peak towards higher masses is a further proof that this peak is not due to the  $f \rightarrow \pi^0 \pi^0$  decay channel (for which  $p_0$  is twice as large as in the case of decay (8) and the peak displacement is negligible) and that  $\eta\eta$  systems have been correctly identified.

The dependence of the  $SD_0$  relative phase  $\alpha$  on the mass  $M_{\eta\eta}$  (Fig. 6c) is in qualitative agreement with the existence of two resonances. It is reproduced with the Breit-Wigner parametrizations of S-wave and D-wave amplitudes (9) and (12) and the fixed masses and widths of the  $f$  and  $G$ . The result is shown on Fig. 7.

## 9. PRODUCTION CROSS-SECTIONS AND BRANCHING RATIOS

The production cross-section at 38 GeV/c of  $G(1590)$  detected through its  $\eta\eta$  decay channel has been determined by comparing the number of events under the  $G$ -peak (Fig. 6a) with the number of  $f \rightarrow \pi^0 \pi^0$  decays ( $\sim 3 \cdot 10^5$ ) observed during the same data taking:

$$\sigma(\pi^- p \rightarrow Gn) \cdot \text{BR}(G \rightarrow \eta\eta) = (33 \pm 8) \text{ nb} \quad (13)$$

where  $\text{BR}(G \rightarrow \eta\eta) = \Gamma(G \rightarrow \eta\eta)/\Gamma(G \rightarrow \text{all})$ . The previously measured cross-section for the reaction  $\pi^- p \rightarrow fn$  ( $\sigma = (5.1 \pm 1.3) \mu\text{b}$ ) [16] has been used for normalization.

The  $t$ -dependence of the  $G(1590)$  production cross-section in reaction (1) is in agreement with OPE dominance (Fig. 8).

The precision on the partial width of decay (8) is essentially determined by the uncertainty of the normalisation procedure based on the decay  $f \rightarrow \pi^0 \pi^0$ . For the decay channel (8) one obtains

$$\text{BR}(f \rightarrow \eta\eta) = (5.2 \pm 1.7) \cdot 10^{-3} \quad (14)$$

The small intensity of this decay is due mainly to the factor  $p_0^5$  [17].

As observed on Fig. 6b, the  $\theta \rightarrow \eta\eta$  resonance does not appear in the D-wave. The upper limit is (95% C.L.):

$$\sigma(\pi^- p \rightarrow \theta n) \cdot \text{BR}(\theta \rightarrow \eta\eta) < 10 \text{ nb} \quad (15)$$

10. NATURE OF THE G(1590)-meson

The small coupling of the G(1590) to pion pair is one of its unusual properties. From the results obtained for the S-wave contribution to reaction (3) in this experiment and the absence of  $G \rightarrow \pi^0 \pi^0$  signal, it follows

$$\text{BR}(G \rightarrow \pi^0 \pi^0) < 0.3 \text{BR}(G \rightarrow \eta \eta) \quad (16)$$

The small value of the G(1590) production cross-section (13) by means of one pion exchange is linked to its small coupling to pion pair. SU(3) symmetry predicts  $\text{BR}(G \rightarrow \pi^0 \pi^0) \approx 1.4 \text{BR}(G \rightarrow \eta \eta)$ .

Another unusual property of the G(1590) is its small coupling to kaon pair. The decay  $G \rightarrow K\bar{K}$  has not been observed in the S-wave contribution to reaction  $\pi^- p \rightarrow K\bar{K}n$  [13,14], so that

$$\text{BR}(G \rightarrow K\bar{K}) < 0.6 \text{BR}(G \rightarrow \eta \eta) \quad (17)$$

This excludes the possibility to consider the G(1590) as a  $s\bar{s}$  state.

The G(1590)-meson could be an hypothetical four quark state of the type  $(u\bar{u} + d\bar{d})s\bar{s}/\sqrt{2}$ . This could explain the reduced two pion decay mode and the large width of the resonance. But in this case one should have  $\text{BR}(G \rightarrow K\bar{K}) = 2 \text{BR}(G \rightarrow \eta \eta)$  [3] in contradiction with (17).

The reduced G(1590) decay rate into  $\pi\pi$  and  $KK$  pairs cannot be explained in a simple way in the frame of the two and four quark schemes. Other explanations must be explored, in particular the possibility of this particle to be a gluonium candidate.

This possibility might resolve another difficulty linked to the existence of three isoscalar mesons ( $S^*(975)$ ,  $\epsilon(1300)$  and  $G(1590)$ ) with  $J^{PC} = 0^{++}$  which cannot together belong to the same SU(3) nonet. One of these could be a gluonium candidate [3] (if, naturally, it will not later be shown that they belong to different nonets)<sup>(\*)</sup>.

---

(\*) Other glueball candidates reported in the litterature, apart from  $\theta$ , are:  $\iota(1440)$  with  $J^{PC} = 0^{-+}$  [18,19,3] and  $g_T(2160)$  and  $g_T(2320)$  with  $J^{PC} = 2^{++}$  [20].

The identification of the G(1590)-meson with the  $\theta$ -meson, another gluonium candidate which also decays into two  $\eta$  mesons, is excluded by their different spins. Furthermore the value of the  $\theta$  mass,  $(1700 \pm 20) \text{ MeV}/c^2$  [4], does not allow to consider it and G(1590) as one and the same particle. Finally, in contradiction with (17),  $BR(\theta \rightarrow K\bar{K}) \approx 3BR(\theta \rightarrow \eta\eta)$ .

## 11. CONCLUSIONS

The main results of this experiment are:

- a new scalar G(1590)-meson has been observed with a mass of  $(1590 \pm 25) \text{ MeV}/c^2$ , a full width of  $(210 \pm 40) \text{ MeV}/c^2$  and quantum numbers  $I^G(J^P)C = 0^+(0^+)_{+}$ ;
- the decay rates of G(1590) into a pair of pions or kaons are depleted in comparison with SU(3) predictions. The experimental observation of these decays could be very important to understand the nature of this particle;
- the properties of G(1590) do not agree with the two quark or four quark schemes. The G(1590) could be interpreted as a gluonium;
- the rare  $f \rightarrow \eta\eta$  decay mode has been simultaneously put in evidence with a branching ratio of 0.5%.

## Acknowledgements

We would like to thank S.S. Gerstein and A.K. Likhoded for discussing our results, and S.N. Grudzin for his help in programming the data analysis. We also thank IHEP and CERN directorates for their support to this experiment.

REFERENCES

- [1] W.D. Apel et al., Preprint IHEP 75-100, Serpukhov (1975); *Yad. Fys.* 28 (1978) 108.
- [2] C. Edwards et al., *Phys. Rev. Letters* 48 (1982) 458.
- [3] D.L. Scharre, SLAC-PUB-2880 (1982); S. Meshkov, CALT-68-923 (1982); J.F. Donoghue, UMHEP -157 (1982) (also for further references).
- [4] E.D. Bloom, SLAC-PUB - 2976 (1982).
- [5] F. Binon et al., *Yad. Fys.* 36 (1982) 670; *Nuovo Cimento* 71A (1982) 497.
- [6] F. Binon et al., *Yad. Fys.* 33 (1981) 1244; *Zeit. Phys. C*, 9 (1981) 109.
- [7] F. Binon et al., *Nucl. Instr. Meth.*, 188 (1981) 507.
- [8] W.D. Apel et al., *Nucl. Phys.* B201 (1982) 197.
- [9] W.D. Apel et al., *Nucl. Phys.* B193 (1981) 269.
- [10] J.L. Petersen, CERN 77-04 (1977) (also for further references).
- [11] W.D. Apel et al., *Phys. Letters* 57B (1975) 398; *Yad. Fys.* 23 (1976) 333.
- [12] L. Gorlich et al., *Nucl. Phys.* B174 (1980) 16.
- [13] B. Cohen et al., *Phys. Rev.* D22 (1980) 2595.
- [14] A. Etkin et al., *Phys. Rev.* D25 (1982) 2246.
- [15] *Rev. Particle Properties*, *Phys. Letters* 111B (1982) 3.
- [16] V.N. Bolotov et al, *Yad. Fys.* 20 (1974) 1214; *Phys. Letters* 52B (1974) 489.
- [17] B.L. Ioffe et al., *JETP* 45 (1965) 375.
- [18] P. Baillon et al., *Nuovo Cimento* 50 A (1967) 393.
- [19] C. Edwards et al., *Phys. Rev. Letters* 49 (1982) 259.
- [20] A. Etkin et al., *Phys. Rev. Letters* 49 (1982) 1620.

FIGURE CAPTIONS

Fig. 1 a) Invariant mass spectrum of  $\gamma$  pairs produced in reaction (2) with multiplicity  $k = 4$ ; b) idem for one of the pairs observed together with the other in the mass interval  $450 \text{ MeV}/c^2 < M_{\gamma_1\gamma_2} < 650 \text{ MeV}/c^2$ , corresponding to the  $\eta$ -meson; c) and d) same as a) and b) respectively, excluding events with  $M_{\gamma_i\gamma_j}$  in the mass interval 90 to 180  $\text{MeV}/c^2$ . Pairs of gammas with a c.m. decay angle  $\theta_0$  such that  $\cos \theta_0 < 0.8$  have been retained only. Displayed events belong to the mass interval  $1500 \text{ MeV}/c^2 < M_{\eta\eta} < 1700 \text{ MeV}/c^2$ . Other mass intervals show similar spectra.

Fig. 2  $t$ -distribution of reaction (1) events in the mass range  $1500 \text{ MeV}/c^2 < M_{\eta\eta} < 1700 \text{ MeV}/c^2$ . Similar distributions are obtained in other mass intervals. The full curve is obtained from  $f$ -mesons produced in the same experiment:  $\pi^-p \rightarrow fn$ ,  $f \rightarrow \pi^0\pi^0$ , a reaction dominated by OPE ( $d\sigma/dt \sim -t(t-m_\pi^2)^{-2}\exp(bt)$ ,  $b \approx 5 (\text{GeV}/c)^{-2}$ ).

Fig. 3 Mass spectrum of  $\eta$  pairs produced in reaction (1).

Fig. 4 Polar angle distribution in the Gottfield-Jackson frame of  $\eta$  pairs produced in reaction (1) for successive mass intervals. The dashed curves represent the detection efficiency  $\epsilon(M_{\eta\eta}, \theta^*)$  integrated over azimuthal angle  $\phi^*$ . The full curve is the distribution in the case of a spin  $J=2$  fully aligned resonance.

Fig. 5 Angular distributions of amplitude  $A$  (dashed curve) and intensity  $N \sim |A|^2$  (full curve) in the case of one pion exchange for several combinations of  $S$  and  $D$  waves.  $x = \cos\theta^*$ . (D) corresponds to a pure  $D$ -wave  $\eta\eta$  state, its amplitude  $A$  is proportional to  $P_2(\cos\theta^*)$ , the second order Legendre polynomial; (D+S) corresponds to a mixing of  $S$  and  $D$  waves in constructive interference; (D-S) is the same for destructive interference.

Figure Captions (Cont'd)

- Fig. 6 Partial waves contributing to reaction (1) in the  $M_{\eta\eta}$  mass region from threshold (indicated by an arrow) up to  $1.9 \text{ GeV}/c^2$ . a) intensity of the S-wave, b) intensity of the  $D_0$ -wave, c) relative phase between S-wave and  $D_0$ -wave, d) depolarisation parameter R for  $\beta = \pi$ , e) phase  $\beta$  for  $R^2$  fixed at 0.4. The full curve on Fig. 6a) is the S-wave obtained with the parametrization (9). The full curve on Fig. 6b) is the  $D_0$ -wave obtained from parametrization (12), the dashed curve is the background contribution ( $\sim p_0^5(M)$ ).
- Fig. 7 Same as on Fig. 6 c). The full curve is the result of a fit with two resonances: G(1590) and f mesons.
- Fig. 8 Integrated t-distribution for the production of a) G(1590)-meson and b) f-meson in reaction (1). The curves correspond to the OPE mechanism (see Fig. 2).

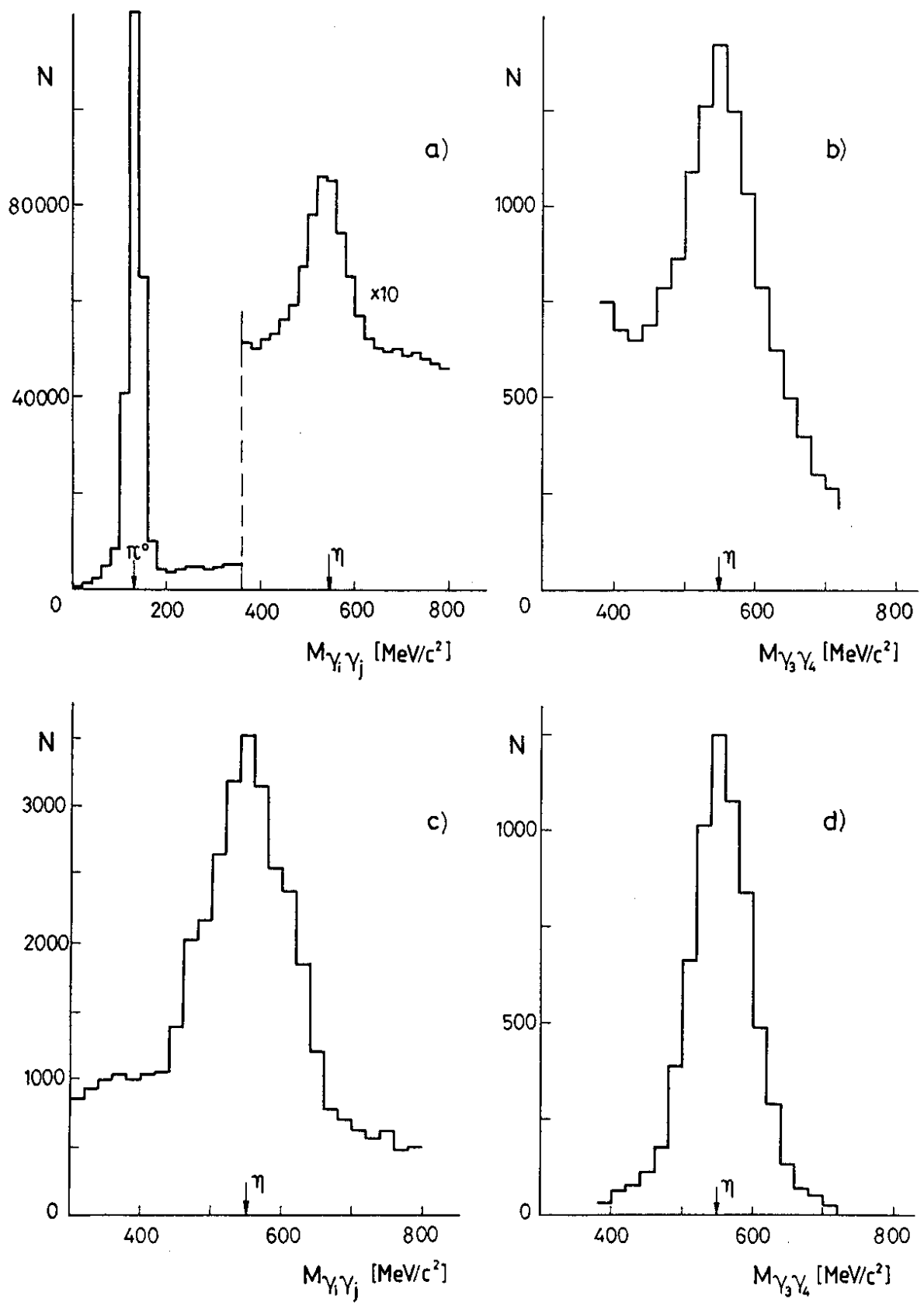


FIG. 1



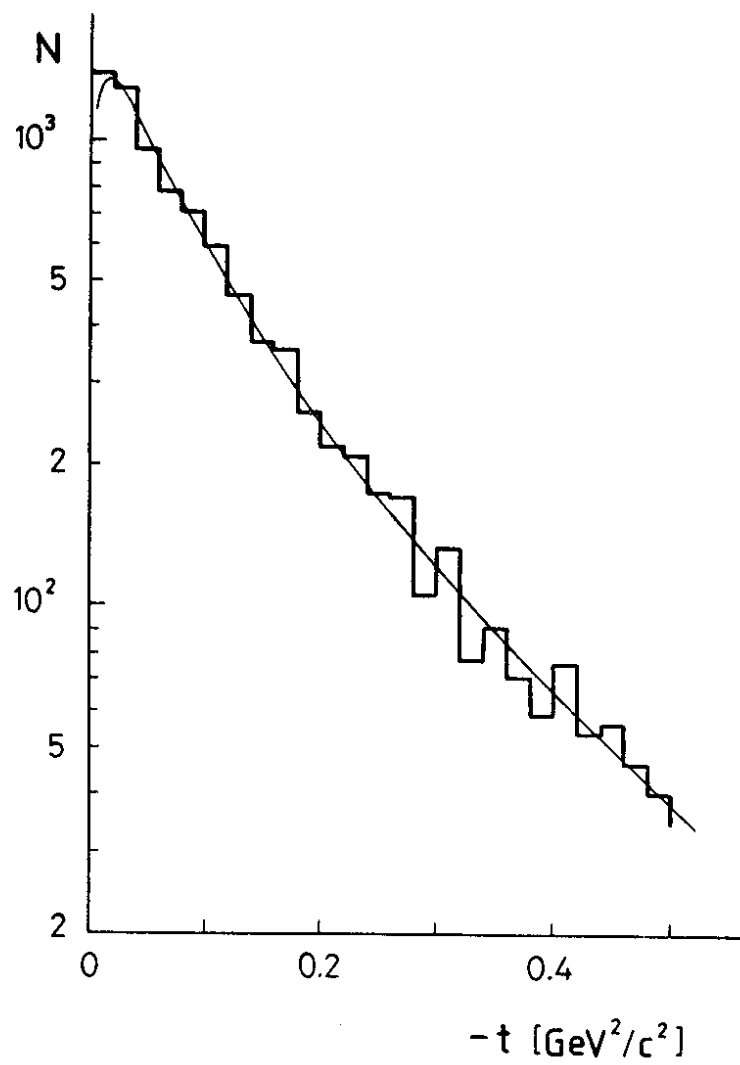


FIG. 2

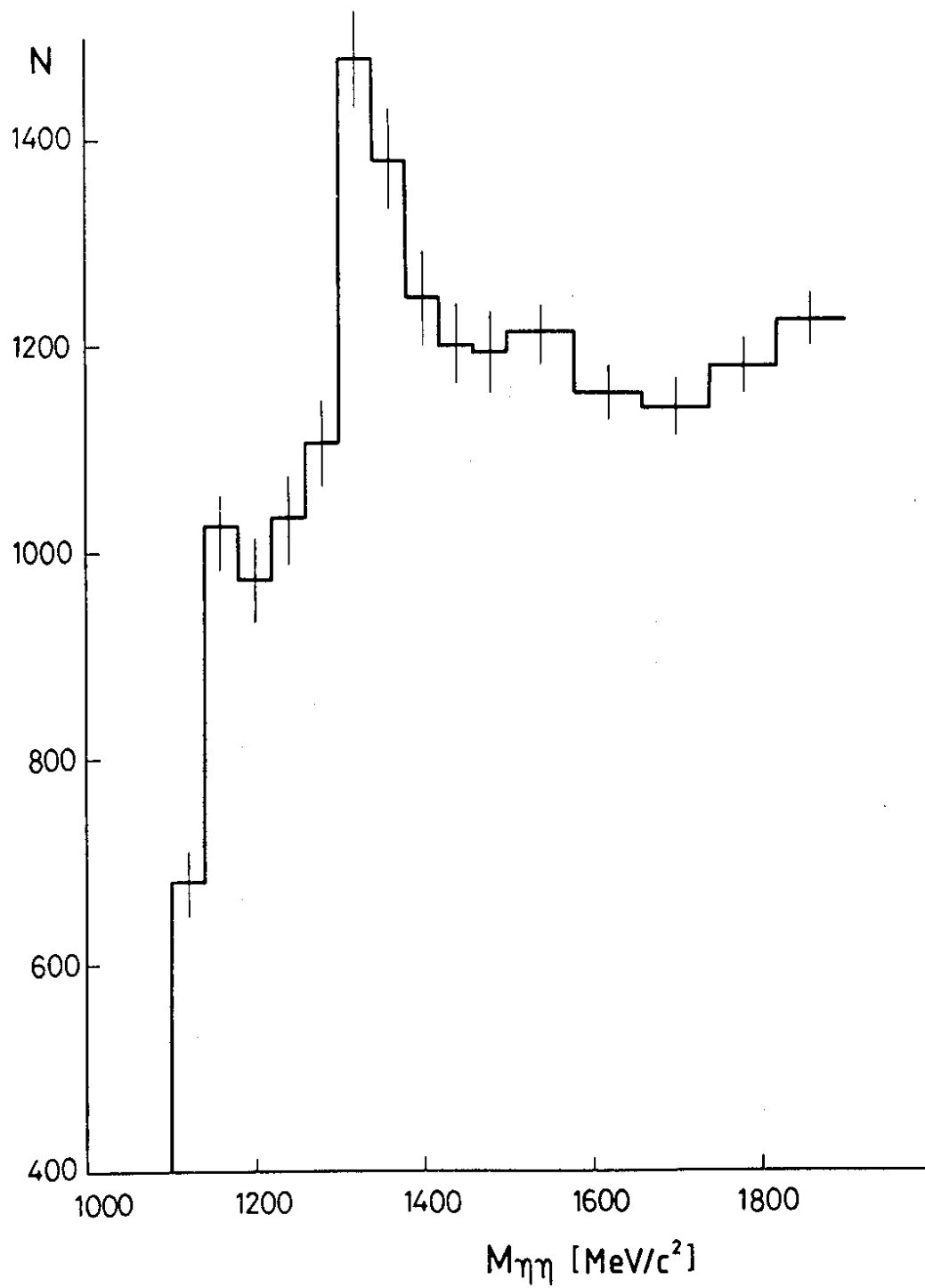


FIG. 3

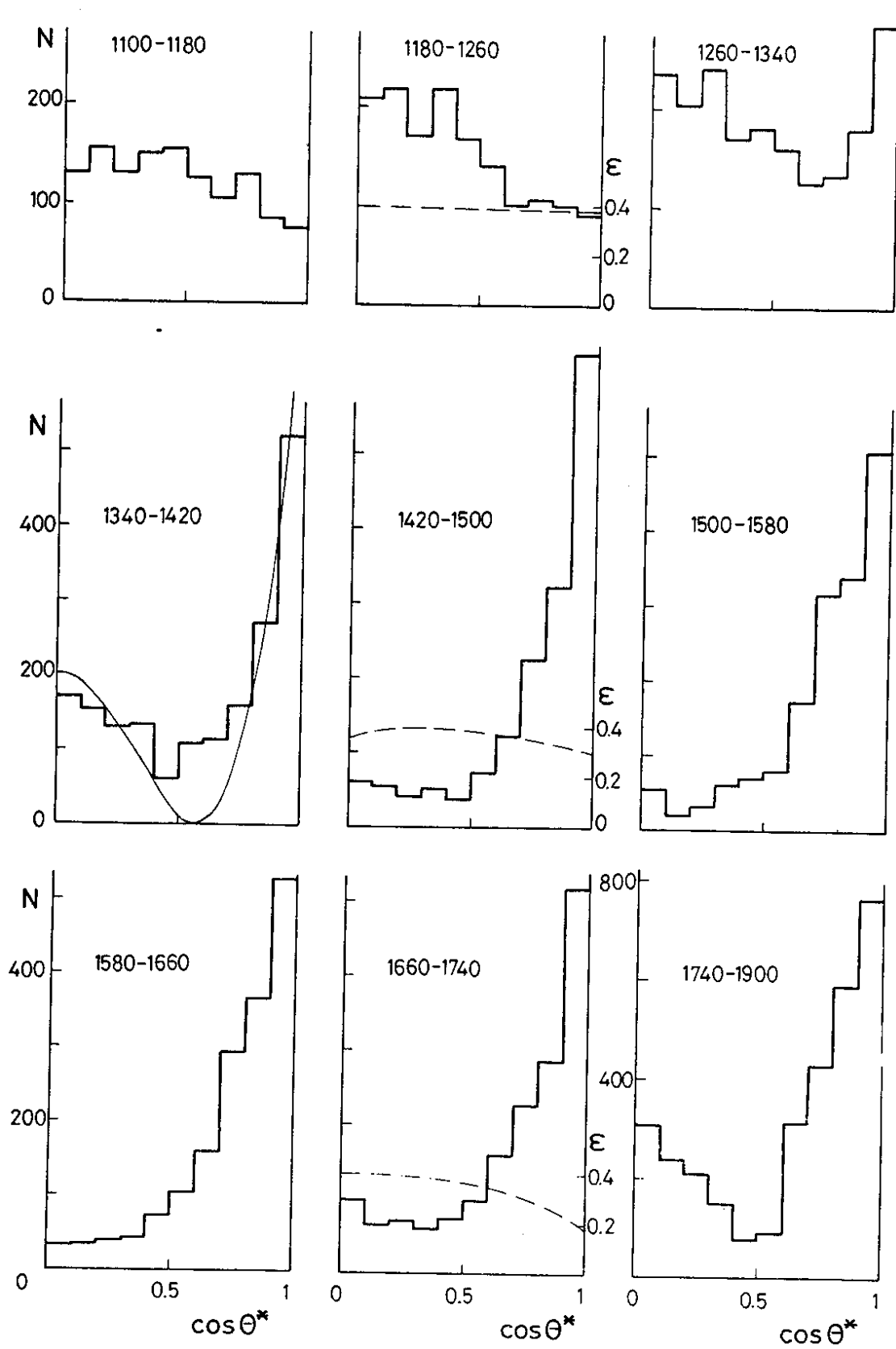


FIG. 4

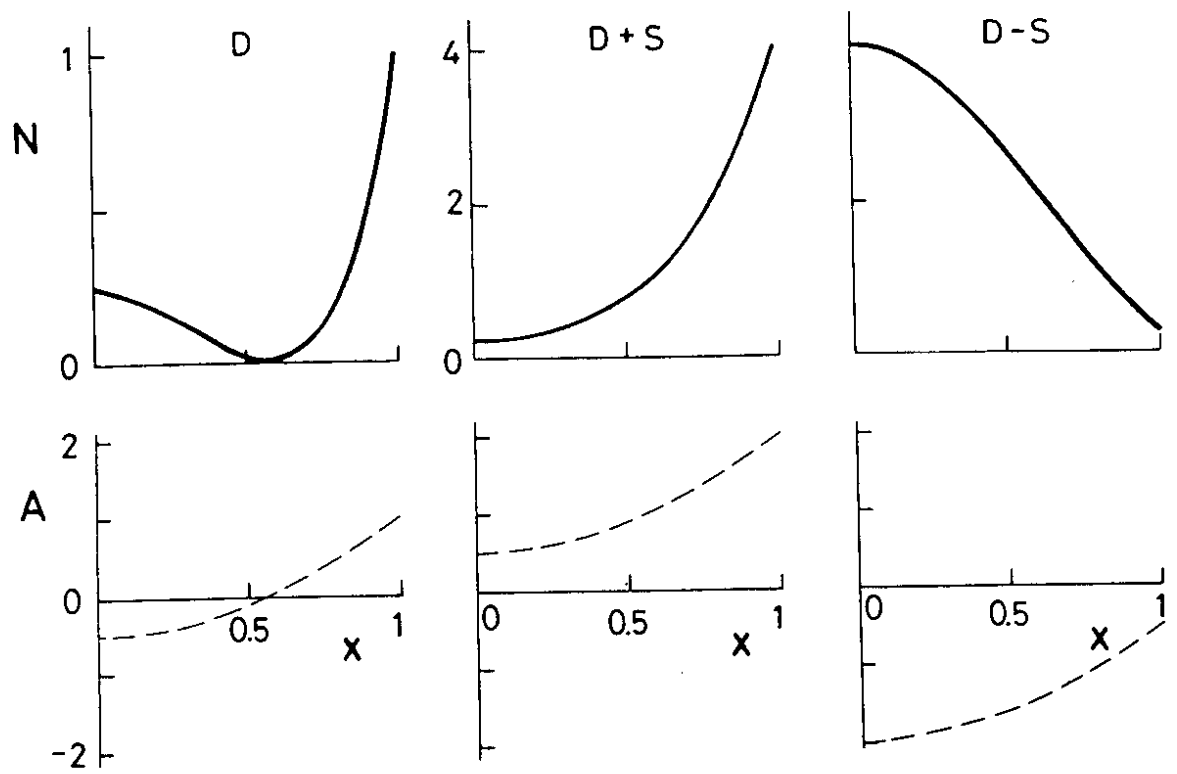


FIG. 5

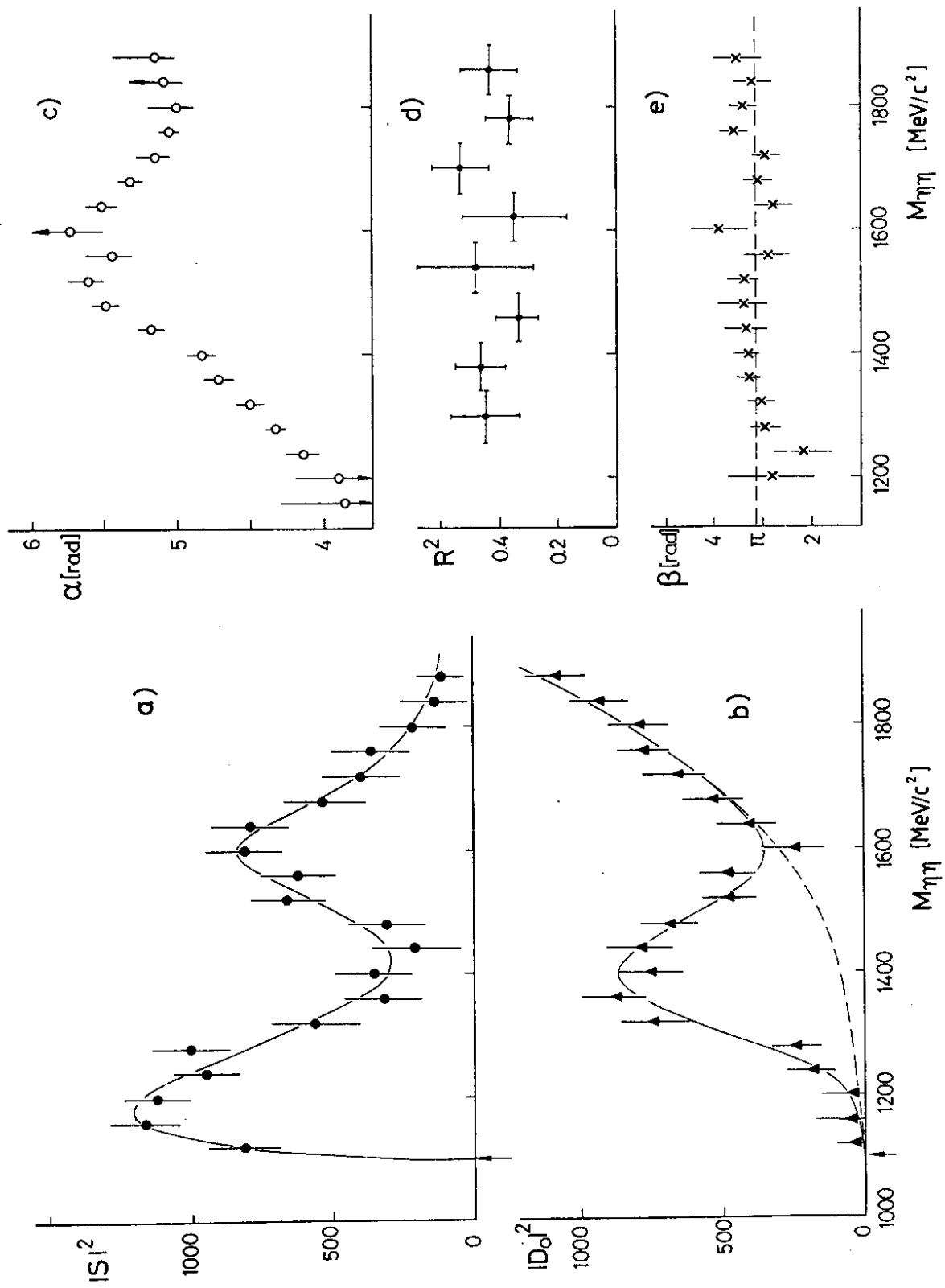


FIG. 6

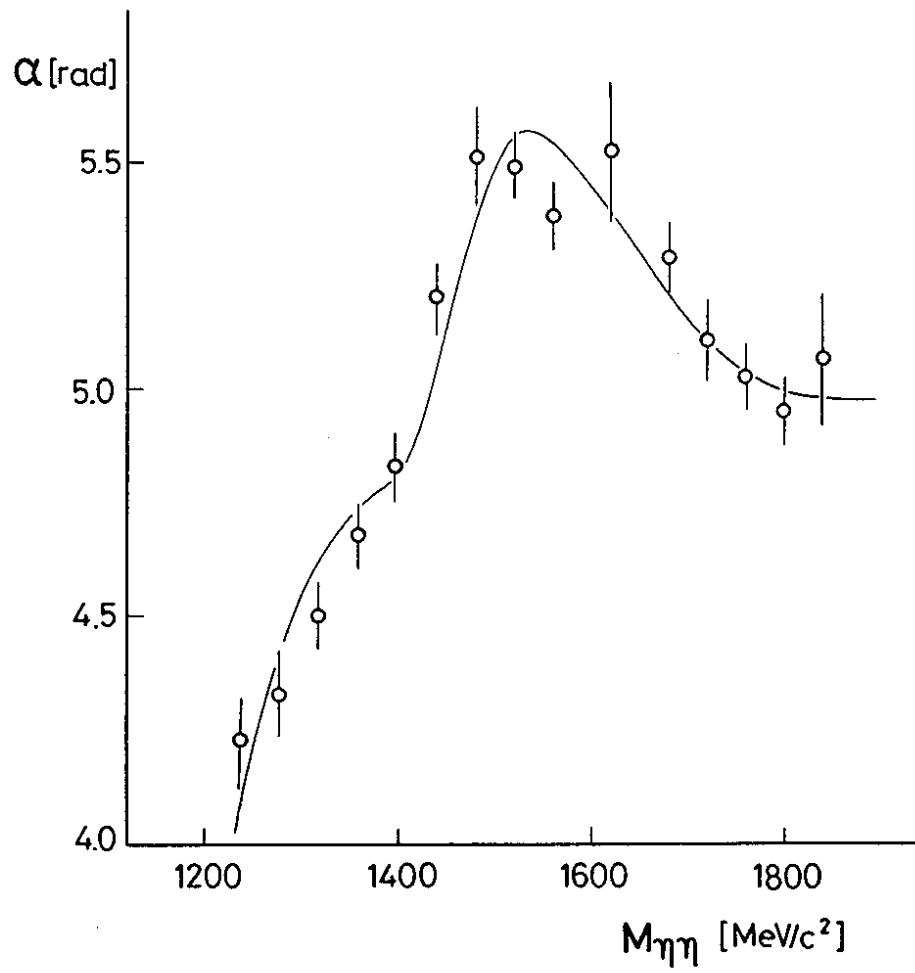


FIG. 7

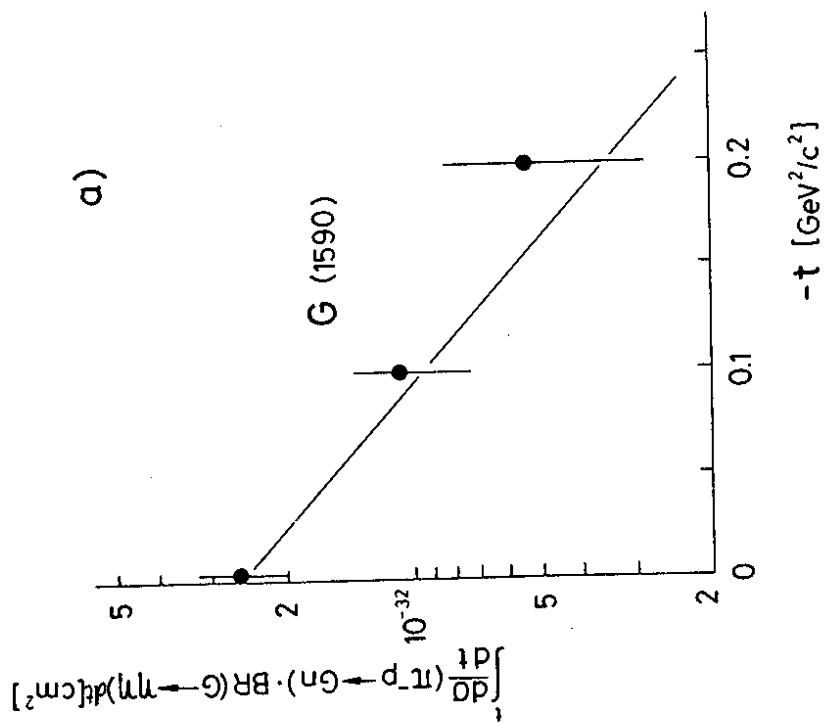
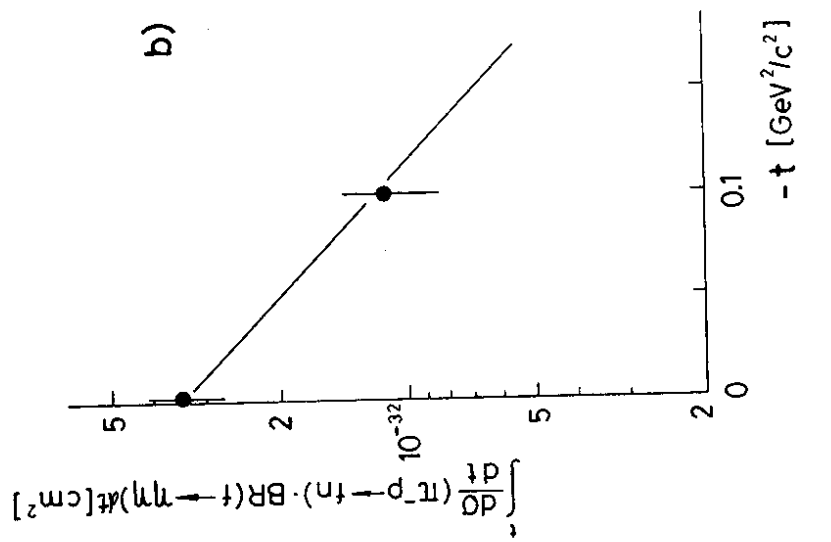


FIG. 8

